ACCSCIENCE PUBLISHING

Eurasian Journal of Medicine and Oncology

ORIGINAL RESEARCH ARTICLE

Comprehensive characterization of the material basis and network pharmacology of Dan-Shen-Yin in the treatment of gastritis

Jianbing Dong[1†], Zhirong Zhou[1†], Yi Chen[2†], Peng Lei[1], Qingrui Zhang[1], and Miaomiao Jiang[1,3*]

[1]National Key Laboratory of Chinese Medicine Modernization, Tianjin University of Traditional Chinese Medicine, Tianjin, China

[2]College of Integrative Medicine, Tianjin University of Traditional Chinese Medicine, Tianjin, China

[3]Science and Technology Project of Haihe Laboratory of Modern Chinese Medicine, Tianjin, China

Abstract

Introduction: Dan-Shen-Yin (DSY), a traditional Chinese medicinal prescription composed of *Salvia miltiorrhiza* Bge. (DS), *Santalum album* L. (TX) and *Amomum villosum* Lour. (SR), has been widely employed in the treatment of gastritis in modern clinical practice and demonstrates excellent therapeutic efficacy. However, the main active ingredient and underlying mechanisms of action remain unclear.

Objective: The aim of this study is to comprehensively characterize the chemical composition of DSY and elucidate its potential mechanisms in the treatment of gastritis.

Methods: The nonvolatile compounds in DSY were analyzed through liquid chromatography-mass spectrometry using the data-dependent acquisition approach, employing an in-house database. The volatile compounds and polysaccharides were detected by gas chromatography-mass spectrometry and high-performance liquid chromatography, respectively. Network pharmacology analysis was performed based on the identified compounds.

Results: A total of 52 nonvolatile and 15 volatile compounds were identified in DSY decoction, primarily including phenylpropanoids, phenols, flavonoids, and terpenoids. Specifically, 54 compounds were found in DS, 14 in SR, and 8 in TX. DSY polysaccharide consisted of seven kinds of monosaccharides, including mannose, rhamnose, glucuronic acid, galacturonic acid, glucose, galactose, and arabinose, with molar percentages of 0.21%, 0.53%, 0.15%, 4.12%, 6.24%, 18.07%, and 0.84%, respectively. Network pharmacology analysis identified 22 key compounds among the 67 compounds detected. These compounds exert the therapeutic effects through 55 core targets (e.g., interleukin-6, tumor necrosis factor, and TP53) and 10 inflammation-related pathways, such as the MAPK and nuclear factor kappa B signaling pathways.

Conclusion: This study further enriches the research on the material basis of DSY and reveals that its volatile compounds, nonvolatile compounds, and polysaccharides contribute to its therapeutic efficacy against gastritis. These findings may facilitate further development and application of DSY in gastritis treatment.

Keywords: Dan-Shen-Yin; Gastritis; Chemical components; Network pharmacology

†These authors contributed equally to this work.

***Corresponding author:**
Miaomiao Jiang
(miaomiaojiang@tjutcm.edu.cn)

Citation: Dong J, Zhou Z, Chen Y, *et al*. Comprehensive characterization of the material basis and network pharmacology of Dan-Shen-Yin in the treatment of gastritis. *Eurasian J Med Oncol*. 2025;9(3):168-184.
doi: 10.36922/EJMO025160124

Received: April 15, 2025

Revised: May 28, 2025

Accepted: June 20, 2025

Published online: July 17, 2025

1. Introduction

Gastritis is an inflammatory condition of the gastric mucosa that can lead to symptoms such as pain, discomfort, and digestive disturbances. It is typically categorized as acute, chronic, or specific gastritis.[1] As a common gastrointestinal disease, gastritis can progress to gastric cancer, one of the most prevalent and lethal malignant tumors in the world.[2,3] Currently, clinical management of gastritis relies on gastric mucosal protection and symptomatic relief, using interventions such as Vitamin C supplements, *Helicobacter pylori* (*H. pylori*) eradication, proton pump inhibitors (PPIs), and non-steroidal anti-inflammatory drugs (NSAIDs).[4] However, the therapeutic effects of vitamin C and NSAIDs in preventing the progression of gastritis to gastric cancer are unclear and are subject to ongoing debate.[4] In addition, Du *et al.*[5] conducted a systematic review and meta-analysis, finding that *H. pylori* eradication therapy are associated with a higher incidence of adverse events during treatment. Moreover, the long-term use of PPIs may increase the risk of gastric atrophy.[6] Therefore, further research into the prevention and management of gastritis is important.

Dan-Shen-Yin (DSY), first documented in Shi Fang Ge Kuo (AD 1801), is a traditional Chinese herbal formula composed of *Salvia miltiorrhiza* Bge. (DS), *Santalum album L.* (TX) and *Amomum villosum Lour.* (SR) in a ratio of 10:1:1, prepared by water. DSY promotes blood circulation, removes blood stasis, promotes *qi*, and relieves pain. It is commonly used in the treatment of gastric and duodenal ulcers, coronary heart disease, and angina pectoris.[7] Clinical studies have shown that DSY exhibits significant therapeutic effects in treating gastritis.[8] Sun *et al.*[9] compared the therapeutic efficacy and safety of PPIs and DSY in the treatment of gastritis, and found that DSY demonstrated a significant advantage in both aspects. Wang *et al.*[10] found that DSY was effective in regulating gastric pepsinogen secretion and alleviating the severity of gastric mucosal lesions. The therapeutic effects were attributed to DSY's modulation of soluble interleukin-2 receptor, tumor necrosis factor alpha (TNF-α), prostaglandin 2 (PGE_2), and calcitonin gene-related peptide, which attenuates mucosal inflammation and protects the gastric mucosa. Moreover, pharmacological studies have confirmed that DSY enhances ulcer healing and bolsters gastric mucosal defense.[11,12] However, the material basis underlying DSY's effects on gastritis remains insufficiently understood, hindering comprehensive insight into its therapeutic mechanisms.

While the pharmacological actions and constituents of DSY in cardiovascular diseases have been well documented,[7,13] research on its active components and mechanisms in gastritis is still limited. The chemical profiles of the individual herbs in DSY—especially the nonvolatile, volatile compounds, and polysaccharides of DS—have been previously studied.[14,15] In contrast, compositional studies of SR and TX are relatively limited, with investigations of their volatile components mainly conducted by gas chromatography-mass spectrometry (GC-MS).[16,17] In addition, although DSY is commonly administered as a decoction in clinical practice, there have been few comprehensive studies on the composition of DSY decoction.

In this study, we aimed to comprehensively characterize the material basis of DSY decoction using multiple analytical techniques to support foundational research on DSY. Nonvolatile compounds were identified using ultra-high performance liquid chromatography (UHPLC)–Orbitrap Exploris MS with a data-dependent acquisition method based on an in-house database. The volatile compounds and polysaccharides were analyzed by headspace GC-MS (HS-GC-MS) and high-performance liquid chromatography (HPLC), respectively. The relative proportions of volatile compounds, nonvolatile compounds, and polysaccharide components in the DSY decoction were also analyzed. Furthermore, the potential mechanisms by which these components exert therapeutic effects on gastritis were analyzed based on network pharmacology and literature-based analysis.

2. Materials and methods

2.1. Reagents and chemicals

DS, SR, and TX were purchased from Beijing Tongrentang Tianjin Hexi Pharmacy and their details are provided in Table 1. Methanol and acetonitrile for liquid chromatography–mass spectrometry (LC-MS) were procured from Thermo Fisher Scientific (USA). Formic acid was obtained from Wilmington Inc. (USA). Acetic acid was purchased from Shanghai Macklin Biochemical Technology (China). Watsons deionized water (Watsons Corp., China) was used in all experiments.

A total of 28 compounds (Table S1)–purchased either from Ichikawa Vikko Biotechnology (China) and

Table 1. Information on TCM prepared pieces.

TCM prepared pieces	Latin name of original plant	Batch number	Producing area
Salviae miltiorrhizae Radix et Rhizoma (Dan Shen, DS)	*Salvia miltiorrhiza* Bge.	210701	Shandong
Amomi fructus (Sha Ren, SR)	*Amomum villosum Lour.*	20210901	Guangxi
Santali albi Lignum (Tan Xiang, TX)	*Santalum album L.*	20210813	Guangdong

Abbreviations: TCM: Traditional Chinese medicine

Shanghai Yuanye Biotechnology (China)–were used as reference compounds, each with a purity exceeding 98%. The Bradford protein concentration kit was obtained from Beyotime Biotechnology (China). 1-Phenyl-3-methyl-5-pyrazolone (PMP; P816062) was purchased from Shanghai Macklin Biochemical Technology (China). Trifluoroacetic acid was purchased from Shanghai Yien Chemical Technology (China). Ammonium acetate was obtained from Sigma-Aldrich (USA).

2.2. Preparation of DSY decoction

DSY is composed of DS, TX, and SR in a 10:1:1 ratio. Initially, DS was extracted using ten times its weight in water by refluxing and boiling for 2 h at 100°C. TX and SR were then added to the DS residue and extracted using eight times the weight of water over low heat for 1 h. The two extracts were combined, concentrated, and dried. Individual extracts of DS, TX, and SR were prepared using the same method.

2.3. HS-GC-MS analysis of DSY decoction

Lyophilized powders of the aqueous extract of DSY, DS, TX, and SR (all passed through a 50-mesh sieve) were accurately weighed for analysis. The equilibration temperature was set at 120°C. The injection port, transfer line, and detector temperatures were set to 130°C, 140°C, and 220°C, respectively. The equilibration time was 15 min, injection time 1 min, and pressure equilibration time 1 min. An HP-5 MS elastic quartz capillary column (30 m × 0.25 mm, 0.25 μm; Agilent Technologies Inc., USA) was used to separate sample, with high-purity helium as the carrier gas. The pre-column pressure was 9.8 psi, and the column flow rate was 1.2 mL/min. Split injection was performed at a 1:20 ratio. The column heating program is provided in Table S2.

The Agilent MassHunter qualitative analysis navigator B.08.00 (Agilent Technologies Inc., USA) equipped with the NIST.17 standard spectral library was utilized for compound identification. Only compounds with both a positive match and reverse match score >80% were retained. The relative abundance of each volatile compound was determined using peak area normalization.

2.4. UHPLC-Orbitrap Exploris MS analysis

Sample powders (DSY, DS, TX, and SR) and 19 reference compounds were dissolved in 80% methanol. The mixture was centrifuged at 12,000 rpm for 10 min at 4°C and the process was repeated once. The resulting supernatant was used for analysis.

UHPLC separation was performed on a Vanquish UHPLC System (Thermo Fisher Scientific, USA) using a Hypersil GOLD column (2.1 mm × 100 mm, 1.8 μm) maintained at 40°C. The binary mobile phase consisted of 0.1% formic acid in water (A) and acetonitrile (B). The gradient elution procedure was as follows: 0 – 2 min, 10 – 15% B; 2 – 3 min, 15 – 26% B; 3 – 6 min, 26 – 28%); 6 – 8 min, 28 – 28% B; 8 – 9 min, 28 – 75% B; 9 – 11 min, 75 – 75% B; 11 – 15 min, 75 – 80% B; 15 – 17 min, 80 – 90% B; 17 – 19 min, 95% B. The injection volume was 2 μL. Mass spectrometric detection was performed using an Orbitrap Exploris 120 (Thermo Fisher Scientific Inc., USA) in both positive and negative ion scanning modes. Data acquisition was conducted using Full MS/dd-MS2 scanning and a predefined DSY precursor ion list. The "if idle pick others" function was turned on.

The precursor ion list was constructed using constituent information on DS, TX, and SR obtained from databases such as CNKI, TCMSP, and Google Scholar. The Xcalibur 4.2 software (Thermo Fisher Scientific Inc., USA) was used to extract information on potential compounds and identification by comparison against an in-house database and reference compounds.

2.5. Characterization of DSY polysaccharides

Lyophilized powders of DSY, DS, TX, and SR (10 g each) were dissolved in 5 mL of distilled water. Then, 20 mL of ethanol was added to the solution. The suspension was incubated at 4°C for 48 h. The precipitated underlayer was dissolved in distilled water and deproteinized using the Sevag method.[18] The crude polysaccharide samples were then lyophilized.

Total sugar content was measured using the phenol-sulfuric acid colorimetric method[19] with D-glucose as the standard at 490 nm. Total uronic acid content was measured using the m-hydroxyphenyl colorimetric method[20] with galacturonic acid as the standard. Protein content was evaluated using the Coomassie Brilliant Blue assay with bovine serum albumin as the standard.[21]

The monosaccharide composition of the samples was analyzed by HPLC with pre-column derivatization. Polysaccharide samples were hydrolyzed with trifluoroacetic acid (TFA) for 6 h at 105°C. Subsequently, 200 μL each of the acid-hydrolyzed sample and monosaccharide standard mixture were accurately aliquoted. The hydrolysates and monosaccharide standard mixture were converted to their PMP derivatives according to the previous method with some modifications[22] The sample and reference standard samples were analyzed using HPLC at 250 nm at 30°C., using a mobile phase of 17% organic phase (acetonitrile) and 83% aqueous phase (0.05 M ammonium acetate). The same procedure was used to analyze reference monosaccharides. The crude DSY polysaccharide powders

were further analyzed using Fourier-transform infrared spectroscopy (FTIR-640IR, VARIAN, USA).

2.6. Network pharmacology analysis

Based on the identified nonvolatile and volatile compounds of DSY decoction, gene targets were obtained from TCMSP (https://tcmspw.com/index.php) and HERB (http://herb.ac.cn) databases. For compounds lacking target information, SMILES strings were obtained from PubChem (https://pubchem.ncbi.nlm.nih.gov/) and used in SwissTargetPrediction (http://www.swisstargetprediction.ch/), retaining the top five predicted targets for each compound. Official gene symbols were standardized using the UniProt (https://www.uniprot.org/) database.

Gene targets associated with human gastritis were identified based on data retrieved from the DisGeNet (http://www.disgenet.org/), GeneCards (https://www.genecards.org/), and MalaCards (www.malacards.org/) databases.

A Venn diagram was generated by importing the compounds and disease targets into the Venny 2.1.0 platform (https://bioinfogp.cnb.csic.es/tools/venny/). The PPI network was constructed using String 11.5 platform (https://www.string-db.org/) with the species set to *Homo sapiens* and confidence threshold set to >0.7. Subsequently, Cytoscape 3.9.1 with the CytoNCA plugin ((https://cytoscape.org/) was used to calculate the topological property parameters of the PPI network, including betweenness centrality, presence centrality, degree, local average connectivity, eigenvector, and network centrality.

The Metascape database (www.metascape.org/) was used to perform Gene Ontology (GO) and Kyoto Encyclopedia of Genes and Genomes (KEGG) pathway enrichment analyses. The p-value threshold of <0.01 was used for statistical significance. The top 10 GO terms and the top 20 KEGG pathways were selected based on ascending order of p-values.

3. Results and discussion

3.1. Optimization of HS-GC-MS analysis conditions

The effects of headspace sampling conditions, including split ratio, equilibrium temperature, and equilibrium time, on the HS–GC–MS analysis of DSY decoction were systematically investigated. Evaluation criteria included the peak areas of the five representative compounds with the highest response values (furfural, bornyl acetate, 2-methoxy-4-vinylphenol, α-santalol, and cis-nuciferol) and the total number of peaks detected under each condition. The examination results are shown in Figure 1 and Figure S1. Based on an overall evaluation of peak shape, peak area, and the number of peaks, the optimal analytical conditions were determined to be a split ratio of 1:20, an equilibrium temperature of 120°C, and an equilibrium time of 15 min.

3.2. Identification of volatile compounds in DSY decoction

A total of 15 volatile compounds were identified in the DSY decoction (Table 2). These compounds included five terpenoids, three furans, three aromatic hydrocarbons, two alcohols, and two ketones. The relative contents of each compound were calculated using peak area normalization. The results indicated that the contents of 1-oxo-di-epicatechuene, 2,4-di-tert-butylphenol, and camphor were present in relatively high concentrations. Comparison with the volatile profiles of individual herbs (Figure 2) revealed that most volatile compounds in DSY originated from DS, with 12 compounds found in both DS and DSY. However, in terms of their relative content, certain volatile compounds–such as diepicedrene-1-oxide and camphor–originating from TX accounted for 47.677% of the total volatile content in DSY. A detailed identification information of the volatile compounds for each individual herb is provided in Table S3 (DS), Table S4 (TX), and Table S5 (SR). I addition, the Soxhlet extraction method was employed to extract volatile oil from the aqueous extracts. However, the extraction yields of DSY, DS, SR, and TX were <0.1%.

These findings suggest that while the majority of identified volatile species are contributed by DS, the dominant contributors by concentration are compounds derived from TX. Liu *et al.*[23] demonstrated that TX facilitates small intestinal transit and accelerates gastric emptying in a murine model. Studies have indicated that prolonged exposure of the gastric mucosa to gastric acid and reduced gastric mucosal resistance may be the primary causes of gastric mucosal lesions.[24] Therefore, the volatile compounds in DSY decoction, particularly those derived from TX, may exert protective effects on the gastric mucosa by enhancing gastric motility and reducing acid retention.

3.3. Optimization of UHPLC-Orbitrap Exploris MS analysis conditions

To improve the accuracy of the systematic characterization of the nonvolatile compounds of DSY decoction, the chromatographic separation conditions and stationary phases were systematically optimized. Each experimental condition was replicated three times. In the mobile phase evaluation (Figure 3), it was observed that the peaks exhibited improved response and separation when 0.1%

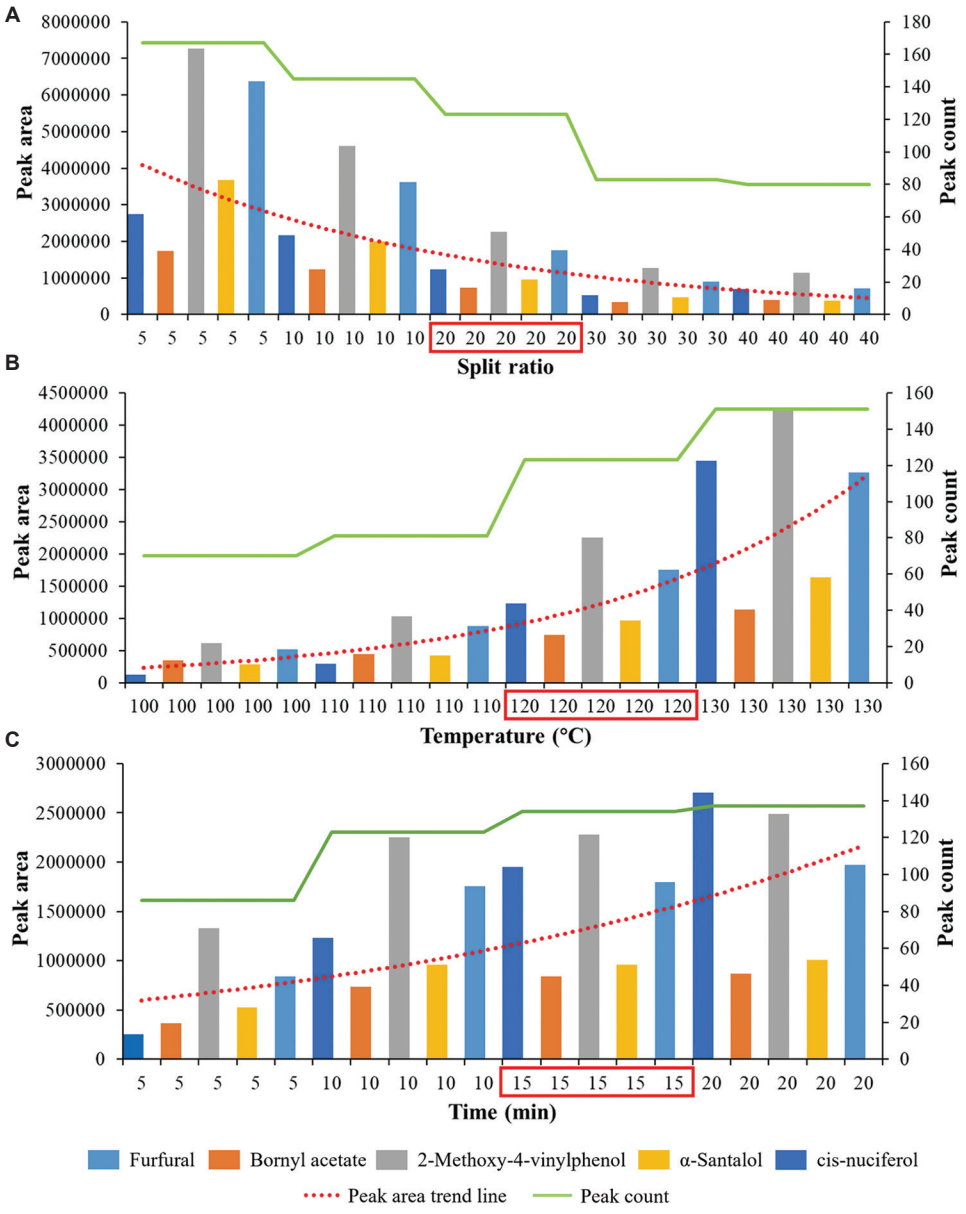

Figure 1. Optimization of GC-MS parameters for DSY decoction analysis. (A) Effect of the split ratio on peak profiles. (B) Effect of the equilibrium temperature on peak profiles. (C) Effect of the equilibrium time on peak profiles.
Abbreviations: GC-MS: Gas chromatography-mass spectrometry; DSY: Dan-Shen-Yin.

formic acid in a water-acetonitrile system was used. In addition, six kinds of chromatographic columns were examined, as shown in Figure 4. The results showed that Hypersil GOLD (Thermo) achieved the best peak separation and yielded the highest number of compounds–totaling 1,436–as determined by SIEVE software extraction in both positive and negative ion modes. Spray voltage, capillary temperature, and auxiliary gas temperature significantly affect the sensitivity and accuracy of mass spectrometry. Therefore, these parameters were optimized in this study, with results as shown in Figure 5. Salvinorin A, salvinorin B, epicatechin, and orientin were used to screen for the optimal spray voltage in the negative ion mode, while dihydrotanshinone I, cryptotanshinone (Cry), and tanshinone IIA were used for the positive ion mode. Based on the peak areas of these compounds, the optimal mass spectrometry parameters were determined as follows: spray voltages of 1.5 kV (positive mode) and 3 kV (negative mode), capillary temperature of 350°C, and auxiliary gas temperature of 400°C.

Table 2. Identification of volatile compounds in DSY decoction based on HS-GC-MS

No.	t_R (min)	Molecular formula	CAS number	Compound name	Match degree		Relative content (%)	Sources
					P. Match	R. Match		
1	4.240	$C_5H_6O_2$	98-00-0	2-Furanmethanol	803	830	1.065	DSY, SR, DS
2	5.444	$C_4H_6O_2$	96-48-0	Butyrolactone	860	966	0.947	DSY, SR, DS
3	8.787	C_8H_8O	122-78-1	Benzeneacetaldehyde	929	959	1.294	DSY, SR, DS
4	9.144	$C_6H_8O_3$	3658-77-3	Furaneol	810	836	0.410	DSY, DS
5	11.568	$C_6H_8O_4$	28564-83-2	4H-pyran-4-one, 2,3-dihydro-3,5-dihydroxy-6-methyl-	921	926	5.750	DSY, SR, DS
6	11.659	$C_{10}H_{16}O$	76-22-2	Camphor	811	906	2.138	DSY, TX
7	15.635	$C_{12}H_{20}O_2$	76-49-3	Bornyl acetate	834	834	0.666	DSY, SR, TX
8	18.588	$C_8H_8O_3$	621-59-0	Isovanillin	817	860	1.166	DSY, DS
9	19.016	$C_{14}H_{26}O_2$	126-86-3	2,4,7,9-Tetramethyl-5-decyn-4,7-diol	822	825	0.818	DSY, DS
10	21.126	$C_{14}H_{22}O$	96-76-4	2,4-Di-tert-butylphenol	938	941	4.684	DSY, DS
11	23.664	$C_{15}H_{26}O$	23811-08-7	Hinesol	854	889	0.565	DSY, DS
12	23.893	$C_{15}H_{26}O$	473-15-4	Beta-eudesmol	885	887	1.467	DSY, DS
13	27.793	$C_{15}H_{28}O_2$	4666-84-6	Cryptomeridiol	844	844	1.472	DSY, DS
14	30.888	$C_{17}H_{24}O_3$	82304-66-3	7,9-Di-tert-butyl-1- oxaspiro (4,5) deca-6,9-diene-2,8-dione	887	891	2.734	DSY, SR, DS
15	31.164	$C_{15}H_{24}O$	/	Diepicedrene-1-oxide	801	810	45.539	DSY, TX

Abbreviations: DS: *Salvia miltiorrhiza Bge.*; DSY: Dan-Shen-Yin; HS-GC-MS: Headspace gas chromatography–mass spectrometry; P.Match: Positive match score; R.Match: Reverse match score; SR: *Amomum villosum Lour.*; TX: *Santalum album L.*; t_R: Retention time.

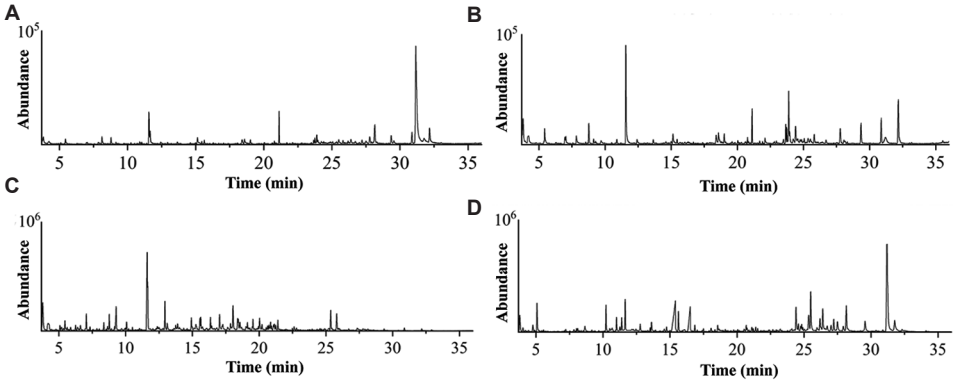

Figure 2. HS-GC-MS TIC diagram for DSY and its individual herbs. (A) DSY. (B) DS. (C) SR. (D) TX
Abbreviations: DS: *Salvia miltiorrhiza Bge.*; DSY: Dan-Shen-Yin; HS-GC-MS: Headspace gas chromatography–mass spectrometry; SR: *Amomum villosum Lour.*; TIC: Total ion chromatogram; TX: *Santalum album L.*

3.4. Identification of nonvolatile compounds in DSY decoction

A precursor ion list consisting of 304 ions (Figure 5D), including 163 $[M+H]^+$ and 141 $[M-H]^-$, was constructed to increase detection sensitivity for trace compounds. Based on reference compounds and an in-house database, 52 nonvolatile compounds in DSY were identified or confirmed through deduction (Figure 6A), including 22 phenylpropanoids, 10 phenols, eight flavonoids, eight diterpenes, two oligosaccharides, a carboxylic acid, and a benzoic acid (Table 3).

In addition, as shown in Figure 6B–D, the nonvolatile compounds in the individual herbs (DS, TX, and SR) were also identified, with details provided in Tables S6–S8. Among the 52 compounds, 42 were derived from DS, mainly phenolic acids such as salvianolic acid A, salvianolic acid B, rosmarinic acid, and lithospermic acid. Eight nonvolatile compounds were derived from SR (three of which were also found in DS), mainly proanthocyanidins. Five nonvolatile compounds were derived from TX, mainly flavonoids. Quantitative analysis of the original aqueous extract indicated that the proportions of nonvolatile components were 70%, 73%, 66.3%, and 55.8% for DSY, DS, TX, and SR, respectively.

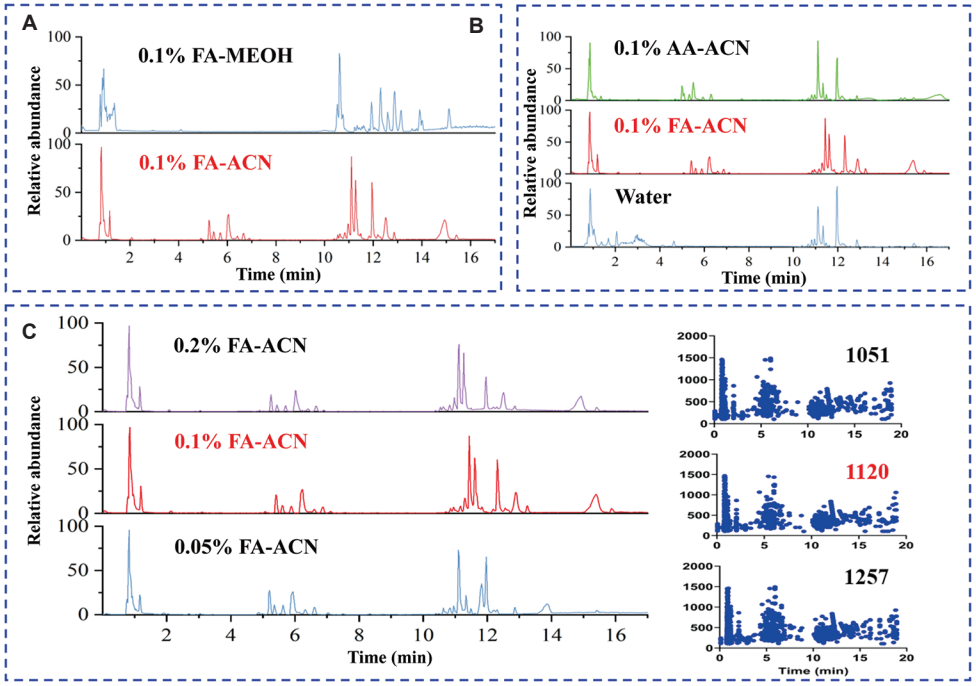

Figure 3. Optimization of mobile phase conditions of UHPLC-Orbitrap Exploris MS analysis. (A) Organic phases. (B) Aqueous phase. (C) Aqueous phase additives.
Abbreviations: AA: Acetic acid; CN: Acetonitrile; FA: Formic acid; MEOH: Methanol; MS: Mass spectrometry; UHPLC: Ultra-high performance liquid chromatography.

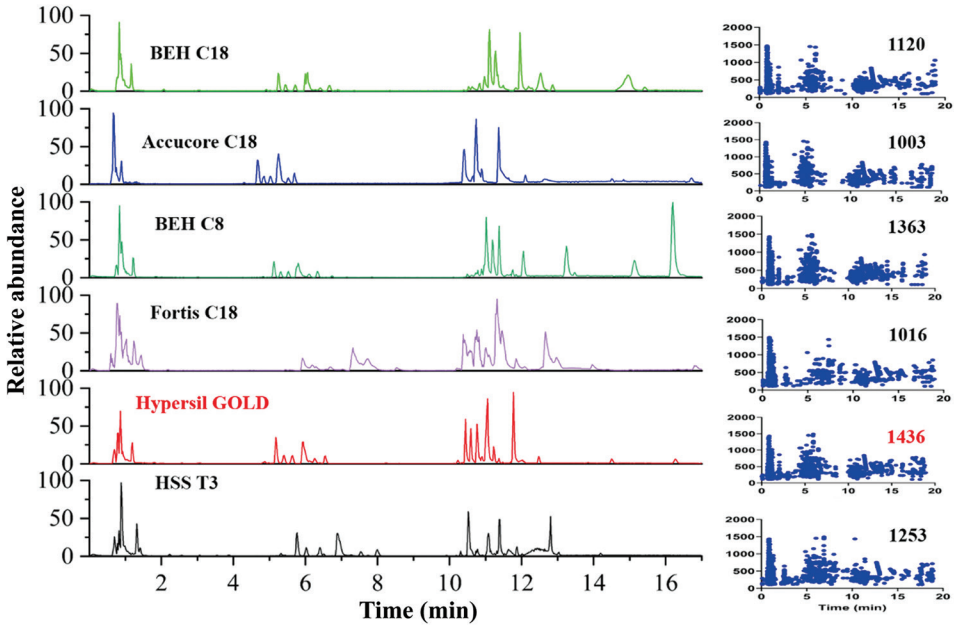

Figure 4. Detection results of UHPLC-Orbitrap Exploris MS analysis using different chromatographic columns
Abbreviations: MS: Mass spectrometry; UHPLC: Ultra-high performance liquid chromatography.

Therefore, the material basis of DSY decoction primarily consists of nonvolatile compounds, the majority of which originate from DS. Modern analytical chemistry and pharmacological studies have demonstrated that DS contains biologically active compounds such as salvianolic acids and tanshinones, which exhibit anti-

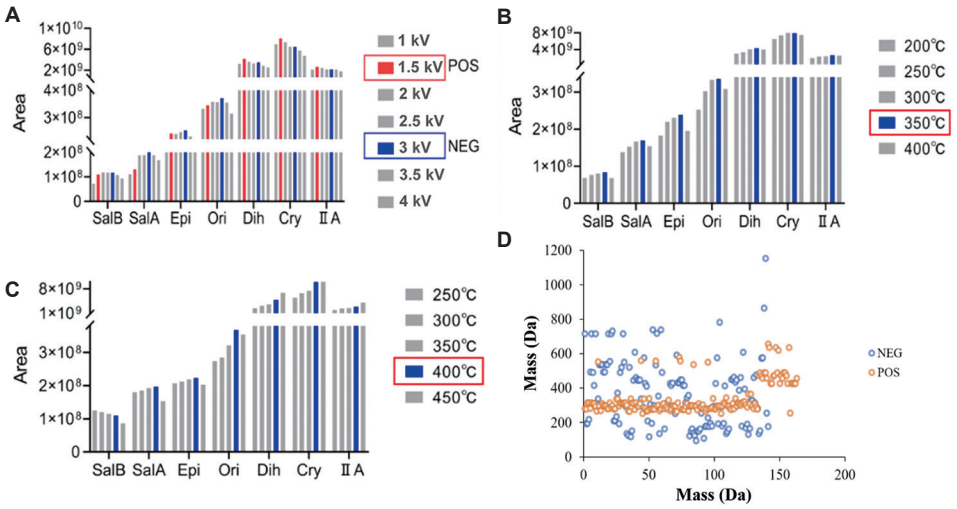

Figure 5. Optimization of key MS parameters for DSY decoction analysis. (A) Effect of spray voltage on peak area. (B) Effect of capillary temperature on peak area. (C) Effect of auxiliary gas temperature on peak area. (D) Distribution map of detected precursor ions in positive and negative ion modes.
Abbreviations: Cry: Cryptotanshinone; Dih: Dihydrotanshinone I; DSY: Dan-Shen-Yin; Epi: Epicatechin; II A: Tanshinone IIA; MS: Mass spectrometry; NEG: Negative ion mode; Ori: Orientin; POS: Positive ion mode; SalA: Salvianolic acid A; SalB: Salvianolic acid B.

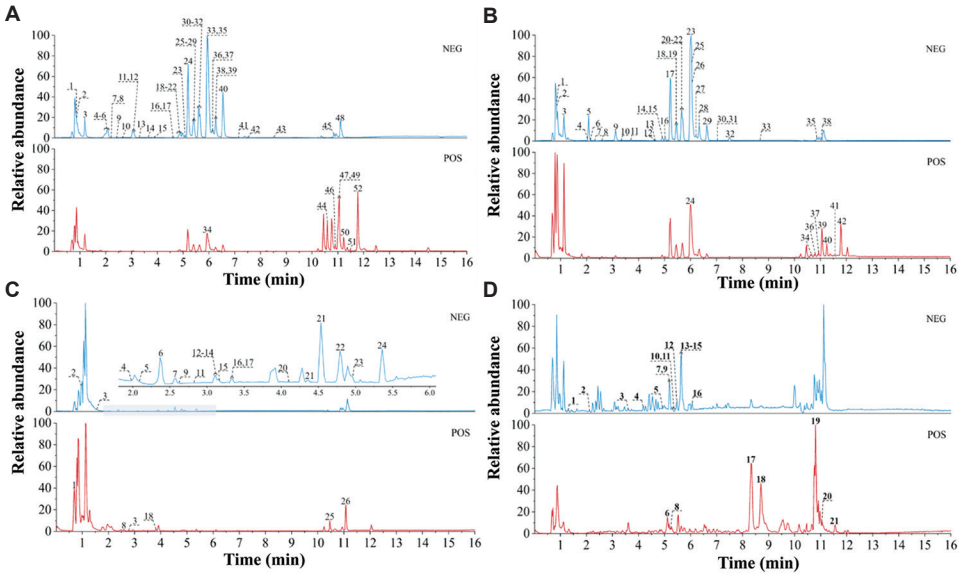

Figure 6. LC-MS TIC diagram positive and negative ion modes for DSY and its individual herbs. (A) DSY. (B) DS. (C) SR. (D) TX.
Abbreviations: DS: *Salvia miltiorrhiza Bge.*; DSY: Dan-Shen-Yin; LC-MS: Liquid chromatography–mass spectrometry; NEG: Negative ion mode; POS: Positive ion mode; SR: *Amomum villosum Lour.*; TIC: Total ion chromatogram; TX: *Santalum album L.*

inflammatory, antioxidant, antitumor, and antimetastatic properties.[25] Moreover, DS extract may serve as a potential chemopreventive agent against bile reflux-associated gastric cancer.[26] Danshensu, a major compound of DS extract, has been shown to prevent bile reflux-induced gastritis and gastric cancer by modulating multiple signaling pathways involved in inflammation, oxidative stress, DNA damage, and apoptosis.[25] Collectively, these findings underscore the significant role of DS-derived nonvolatile compounds in the treatment of gastritis and the prevention of gastric cancer.

3.5. Measurement and analysis of polysaccharides in DSY decoction

The contents of total sugar, uronic acid, and protein in DSY decoction and its individual herbs (DS, TX, and SR) are summarized in Figure 7. The sugar content in DSY was 45.70%, as determined using the phenol-sulfuric acid

Table 3. Identification of nonvolatile compounds in DSY decoction based on UHPLC-Orbitrap Exploris MS

No.	t_R (min)	Mass (ppm)	Molecular formula	Selected ion	ESI-MS^2 fragments	Compound name	Mass error (ppm)	Sources
1	0.83	665.2148	$C_{24}H_{42}O_{21}$	$[M-H]^-$	485.1528, 383.1202, 341.1098	Tetrose	1.948	DSY, DS
2	0.85	341.1090	$C_{12}H_{22}O_{11}$	$[M-H]^-$	179.0565	Disaccharide	3.436	DSY, DS
3	1.12	191.0197	$C_6H_8O_7$	$[M-H]^-$	173.0093, 111.0088	Citric acid	5.607	DSY, DS
4	1.92	329.0879	$C_{14}H_{18}O_9$	$[M-H]^-$	269.0666, 209.0457, 167.0351	Vanillin hexoside	0.166	DSY, SR
5	2.06	151.0402	$C_8H_8O_3$	$[M-H]^-$	123.0453	2-Anisic acid	8.272	DSY, DS
6	2.07	197.0455	$C_9H_{10}O_5$	$[M-H]^-$	179.0352, 135.0453, 123.0453, 72.9932	Danshensu*	−0.135	DSY, DS
7	2.16	151.0402	C8H8O3	$[M-H]^-$	136.0166	Vanillin	0.944	DSY, TX
8	2.18	167.0350	$C_8H_8O_4$	$[M-H]^-$	152.0114, 123.0452, 108.0217, 91.0191	Vanillic acid	0.287	DSY, SR
9	2.35	153.0193	$C_7H_6O_4$	$[M-H]^-$	109.0295, 91.0191	Protocatechuic acid	−0.274	DSY, DS, SR
10	2.63	181.0506	$C_9H_{10}O_4$	$[M-H]^-$	163.0402, 135.0453	3,4-Dihydroxyhydrocinnamic acid	7.538	DSY, DS
11	3.04	289.0710	$C_{15}H_{14}O_6$	$[M-H]^-$	245.0811, 205.0498, 151.0394, 123.0448, 109.0292	Epicatechin*	−2.807	DSY, SR
12	3.06	137.0245	$C_7H_6O_3$	$[M-H]^-$	119.0139, 108.0218, 91.0190	Protocatechualdehyde	0.273	DSY, DS, SR
13	3.27	193.0506	$C_{10}H_{10}O_4$	$[M-H]^-$	149.0608	Ferulic acid*	0.425	DSY, DS
14	3.63	179.0349	$C_9H_8O_4$	$[M-H]^-$	135.0436, 107.0487	Caffeic acid	−0.123	DSY, DS
15	3.81	289.0718	$C_{15}H_{14}O_6$	$[M-H]^-$	245.0811, 205.0494, 123.0447, 109.0291	Catechin*	0.064	DSY, SR
16	4.54	537.1043	$C_{27}H_{22}O_{12}$	$[M-H]^-$	493.1135, 295.0611, 185.0244, 109.0295	Salvianolic acid H	2.788	DSY, DS
17	4.58	313.0718	$C_{17}H_{14}O_6$	$[M-H]^-$	313.0717, 269.0821, 203.0352, 159.0453, 109.0296	Salvianolic acid F	0.059	DSY, DS
18	4.71	537.1043	$C_{27}H_{22}O_{12}$	$[M-H]^-$	493.1135, 295.0611, 185.0244, 109.0295	Salvianolic acid I	0.057	DSY, DS
19	4.86	431.0999	$C_{21}H_{20}O_{10}$	$[M-H]^-$	341.0645, 311.0563, 228.1595, 203.0871	Vitexin*	3.572	DSY, TX
20	4.90	493.1143	$C_{26}H_{22}O_{10}$	$[M-H]^-$	295.0612, 185.0244, 109.0295	Salvianolic acid A*	0.547	DSY, DS
21	4.91	537.1042	$C_{27}H_{22}O_{12}$	$[M-H]^-$	493.1135, 295.0611, 109.0295	Salvianolic acid U	0.634	DSY, DS
22	4.94	463.0884	$C_{21}H_{20}O_{12}$	$[M-H]^-$	300.0276, 271.0249, 243.0295, 151.0039	Quercitrin*	0.326	DSY, SR
23	5.00	537.1041	$C_{27}H_{22}O_{12}$	$[M-H]^-$	493.1135, 295.0611, 109.0295	Salvianolic acid T	0.392	DSY, DS
24	5.21	417.0829	$C_{20}H_{18}O_{10}$	$[M-H]^-$	197.0444, 175.0388	Salvianolic acid D*	0.408	DSY, DS
25	5.34	447.0944	$C_{21}H_{20}O_{11}$	$[M-H]^-$	332.0856, 228.1654, 203.0869	Orientin*	2.472	DSY, TX
26	5.37	447.0939	$C_{21}H_{20}O_{11}$	$[M-H]^-$	300.0278, 271.0252, 255.0303, 243.0298, 151.0039	Isoquercitrin	0.281	DSY, SR
27	5.38	447.0944	$C_{21}H_{20}O_{11}$	$[M-H]^-$	332.0856, 228.1654, 203.0869	Isoorientin*	0.773	DSY, TX
28	5.39	551.1198	$C_{28}H_{24}O_{12}$	$[M-H]^-$	353.0668, 321.0405	Monomethyl lithospermate	0.564	DSY, DS
29	5.44	717.1459	$C_{36}H_{30}O_{16}$	$[M-H]^-$	519.0937, 339.0511, 321.0405	Salvianolic acid B or its isomer	−0.234	DSY, DS
30	5.56	537.1041	$C_{27}H_{22}O_{12}$	$[M-H]^-$	493.1135, 295.0611, 185.0244, 109.0295	Salvianolic acid J	2.565	DSY, DS
31	5.66	359.0772	$C_{18}H_{16}O_8$	$[M-H]^-$	197.0444, 197.0444, 161.0230	Rosmarinic acid*	−0.002	DSY, DS
32	5.79	493.1142	$C_{26}H_{22}O_{10}$	$[M-H]^-$	295.0611, 185.0243, 109.0295	Salvianolic acid A or its isomer	0.365	DSY, DS
33	5.98	717.1460	$C_{36}H_{30}O_{16}$	$[M-H]^-$	295.0606, 519.0930, 339.0503, 321.0399	Salvianolic acid B or its isomer	−0.150	DSY, DS
34	5.99	339.0511	$C_{18}H_{12}O_7$	$[M+H]^-$	295.0615, 185.0244, 109.0295	Salvianolic acid G	0.262	DSY, DS
35	6.01	537.1041	$C_{27}H_{22}O_{12}$	$[M-H]^-$	493.1135, 295.0611, 185.0244, 109.0295	Lithospermic*	2.434	DSY, DS

(Cont'd...)

Table 3. *(Continued)*

No.	t_R (min)	Mass (ppm)	Molecular formula	Selected ion	ESI-MS² fragments	Compound name	Mass error (ppm)	Sources
36	6.06	431.0999	$C_{21}H_{20}O_{10}$	$[M-H]^-$	341.0645, 311.0563, 228.1595, 203.0871	Isovitexin*	3.572	DSY, TX
37	6.07	493.1142	$C_{26}H_{22}O_{10}$	$[M-H]^-$	295.0612, 185.0244, 109.0295	Salvianolic acid A or its isomer	0.304	DSY, DS
38	6.21	717.1459	$C_{36}H_{30}O_{16}$	$[M-H]^-$	519.0937, 339.0511, 321.0405	Salvianolic acid E	1.295	DSY, DS
39	6.33	717.1462	$C_{36}H_{30}O_{16}$	$[M-H]^-$	519.0937, 339.0511, 321.0405	Salvianolic acid B*	0.184	DSY, DS
40	6.64	493.1141	$C_{26}H_{22}O_{10}$	$[M-H]^-$	295.0612, 185.0244, 109.0295	Salvianolic acid A or its isomer	0.243	DSY, DS
41	7.16	493.1142	$C_{26}H_{22}O_{10}$	$[M-H]^-$	295.0611, 185.0243, 109.0295	Salvianolic acid A or its isomer	0.487	DSY, DS
42	7.50	491.0986	$C_{26}H_{20}O_{10}$	$[M-H]^-$	293.0455, 265.0506, 197.0455	Isosalvianolic acid C*	0.468	DSY, DS
43	8.65	491.0986	$C_{26}H_{20}O_{10}$	$[M-H]^-$	293.0455, 249.0555, 135.0451	Salvianolic acid C	0.529	DSY, DS
44	10.57	311.1277	$C_{19}H_{18}O_4$	$[M+H]^-$	267.1377, 203.0853	Tanshinaldehyde	-3.929	DSY, DS
45	10.80	327.1238	$C_{19}H_{20}O_5$	$[M-H]^-$	283.1340, 239.1441	1S-hydroxy-anhydride of 16Rcryptotanshinone	0.040	DSY, DS
46	10.83	311.1277	$C_{19}H_{18}O_4$	$[M+H]^-$	293.1191, 275.1058, 203.0852	Tanshinone IIB	−0.307	DSY, DS
47	10.94	309.1119	$C_{19}H_{16}O_4$	$[M+H]^-$	265.1223, 223.0755, 203.0854	Salvianolic aldehyde	−0.438	DSY, DS
48	11.03	313.1445	$C_{19}H_{22}O_4$	$[M-H]^-$	269.1543, 213.0914	Neocryptotanshinone*	−0.008	DSY, DS
49	11.04	297.1484	$C_{19}H_{20}O_3$	$[M+H]^-$	253.1586, 203.0853	Isocryptotanshinone	−0.674	DSY, DS
50	11.23	279.1014	$C_{18}H_{14}O_3$	$[M+H]^-$	261.0907, 203.0852	Dihydrotanshinone I*	−0.469	DSY, DS
51	11.51	295.1327	$C_{19}H_{18}O_3$	$[M+H]^-$	267.1379, 249.1266, 203.0853	Tanshinone IIA*	−4.431	DSY, DS
52	11.79	297.1482	$C_{19}H_{20}O_3$	$[M+H]^-$	279.1378, 203.0852	Cryptotanshinone*	−4.704	DSY, DS

Note: *Compared with reference compounds.

Abbreviations: DS: *Salvia miltiorrhiza Bge.*; DSY: Dan-Shen-Yin; ESI-MS2: Electrospray ionization tandem mass spectrometry; MS: Mass spectrometry; SR: *Amomum villosum Lour.*; TX: *Santalum album L.*; t_R: Retention time; UHPLC: Ultra-high performance liquid chromatography.

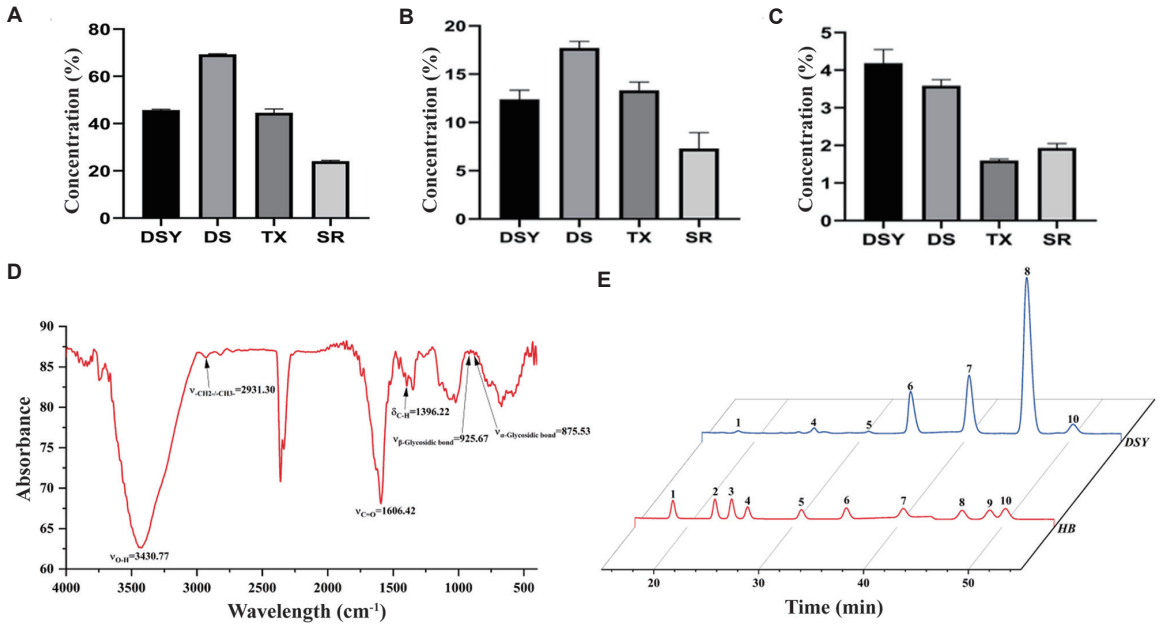

Figure 7. HPLC analysis of monosaccharide compositions of DSY decoction. (A) Total sugar content (mg/g). (B) The total uronic acid content (mg/g). (C) Total protein content (mg/g). (D) Infrared spectrum of the DSY polysaccharide. (E) HPLC chromatogram of the monosaccharide composition of DSY (1: Man 2: Lyx 3: Rib 4: Rha 5: GlcA 6: GalA 7: Glc 8: Gal 9: Xyl 10: Ara HB: Mixed standard).

Abbreviations: Ara: Arabinose; DS: *Salvia miltiorrhiza Bge.*; DSY: Dan-Shen-Yin; Gal: Galactose; GalA: Galacturonic acid; Glc: Glucose; GlcA: Glucuronic acid; HPLC: High performance liquid chromatography; Man: Mannose; Rha: Rhamnose; SR: *Amomum villosum Lour.*; TX: *Santalum album L.*

method. The contents of total uronic acid and proteins in DSY samples were 12.39% and 4.18%, respectively.

The monosaccharide composition of DSY polysaccharide was analyzed using complete acid hydrolysis followed by PMP derivatization and HPLC analysis. As shown in Figure 7D, seven kinds of monosaccharides were identified, including mannose, rhamnose, glucuronic acid, galacturonic acid, glucose, galactose, and arabinose. In addition, the molar percentages of monosaccharide composition were calculated based on their respective peak areas (Table 4). The results revealed that DSY polysaccharide is primarily composed of galactose, glucose, and galacturonic acid.

FTIR spectroscopy (Figure 7E) confirmed the presence of characteristic polysaccharide functional groups. The O–H stretching vibration at 3431 cm^{-1} indicates intermolecular hydrogen bonding. The peak at 2931 cm^{-1} corresponds to $–CH_2–$ or $–CH_3$ stretching vibrations, while the strong absorption at 1606 cm^{-1} indicates the C=O stretch of free carboxyl groups. The peaks at 1396 cm^{-1}, 926 cm^{-1}, and 871 cm^{-1} are assigned to C–H bending, β-glycosidic, and α-glycosidic bonds, respectively. These results are consistent with typical features of plant-derived polysaccharides.

The relative contents of crude polysaccharides in their respective aqueous extracts were 9.8% (DSY), 12.4% (DS), 16% (SR), and 6.4% (TX), indicating that polysaccharides are important components of DSY, primarily derived from SR and DS.

Although polysaccharide macromolecules have complex structures and poor oral absorbability, studies have found that plant polysaccharides can exhibit biological effects in the gastrointestinal tract.[27] DS polysaccharides have been shown to regulate the gut microbiota homeostasis.[28] Moreover, the findings of Gao *et al.*[29] suggest that disruption of the gut microbiota may be a key factor contributing to the worsening of gastric mucosal inflammation, and that restoring gut microbiota balance could be a significant approach to curing or preventing the progression from chronic atrophic gastritis to gastric cancer. In addition, Liu *et al.*[30] found that purified SR polysaccharide (AVLP-2) improved the oxidative stress status of the gastric mucosa by increasing superoxide dismutase activity and glutathione levels and inhibiting malondialdehyde accumulation. Therefore, in the treatment of gastritis, the polysaccharide of DSY may play a significant role. Despite this, polysaccharides have garnered limited attention in previous gastritis studies investigating DSY's mechanisms of action.

3.6. Network pharmacology analysis

A total of 1138 targets related to 67 compounds (15 volatile and 52 nonvolatile) were obtained through the TCMSP, HERB, and SwissTargetPrediction databases. Concurrently, 1719 targets related to gastritis were obtained through the DisGeNet, GeneCards, and MalaCards databases. Venn diagram analysis (Figure 8A) revealed 195 overlapping targets, representing potential therapeutic targets of DSY for treating gastritis. Subsequently, the compounds identified in DSY decoction and these overlapping targets were imported into Cytoscape 3.9.1 to construct a compound–target–disease interaction network (Figure 8B). Network topology parameters–degree, betweenness centrality, and closeness centrality value–were used to evaluate node importance in the network. As shown in Table 5, 22 compounds (5 volatile and 17 nonvolatile) exhibited values greater than the corresponding median values, suggesting their potential as key bioactive components of DSY in treating gastritis.

The shared targets DSY compounds and gastritis were imported to the STRING database, resulting in a PPI network containing 194 nodes and 1142 edges (Figure 8C). The CytoNCA plugin in Cytoscape was then used to assess the importance of each node. Filtering conditions were set as follows: betweenness centrality ≥median, closeness centrality ≥median, degree ≥median, local average connectivity ≥median, eigenvector ≥median, and network ≥median. Ultimately, 55 core targets, including TNF, IL2, IL6, AKT1, STAT3, and TP53, were screened from the 195 intersecting targets (Figure 8C).

The GO enrichment analysis of these 55 core targets returned 1373 terms, including 1234 biological processes, 52 cellular components, and 87 molecular functions. The top 10 terms in each category are shown in Figure 8D. In the biological process category, the therapeutic effects of DSY appear to involve a response to reactive oxygen species. Membrane raft, transcription regulator complex, side of membrane, and endoplasmic reticulum lumen were enriched in the cellular component category. In the molecular function category, protein kinase binding, DNA-

Table 4. Molar percentages of monosaccharide composition in DSY polysaccharide.

Monosaccharide	Mannose	Rhamnose	Glucuronic acid	Galacturonic acid	Glucose	Galactose	Arabinose
Molar %	0.21	0.53	0.15	4.12	6.24	18.07	0.84

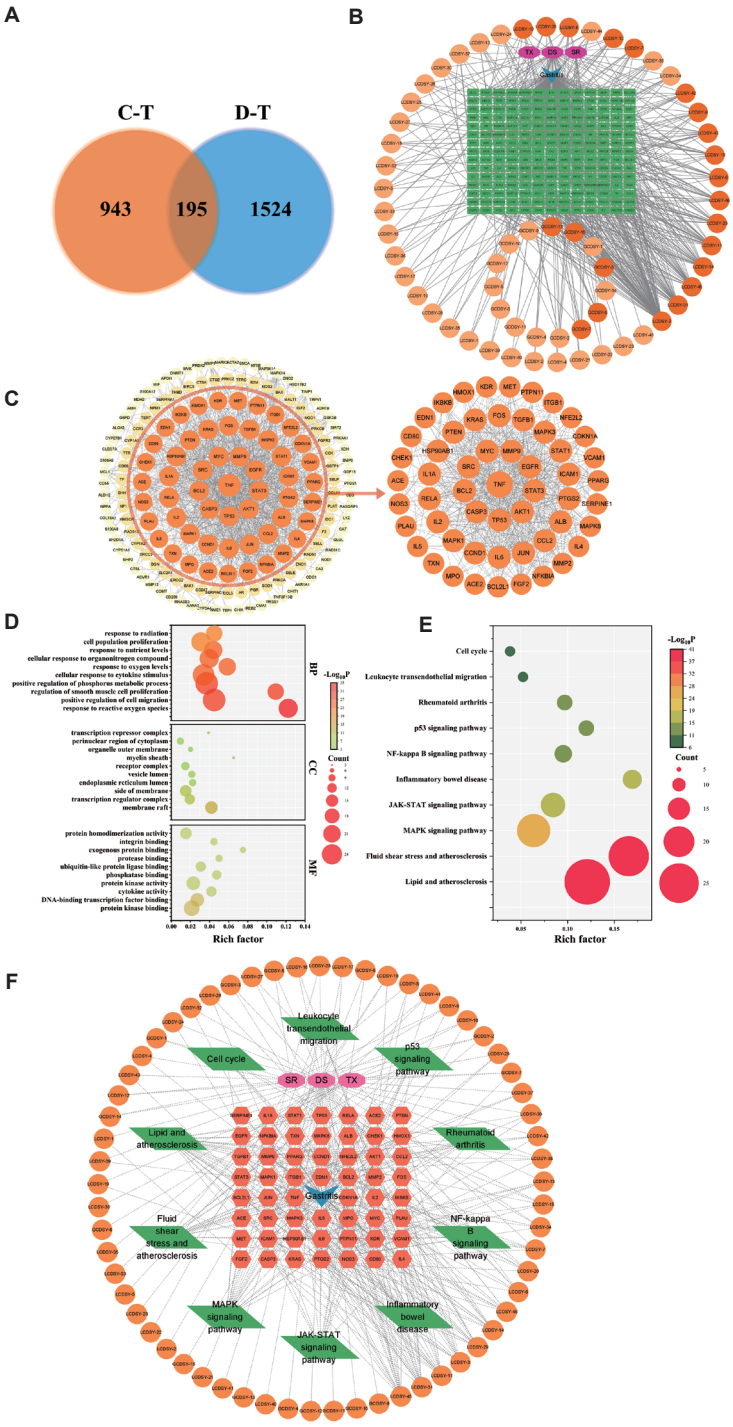

Figure 8. Network pharmacology-based prediction of the mechanisms of DSY in treating gastritis. (A) Venn diagram showing overlapping targets between DSY-related compounds and gastritis-related genes. (B) PPI network and core targets. (C) Compounds-potential targets-disease network. (D) Disease-core targets-compounds-pathways interaction network. (E) GO enrichment analysis of biological processes, molecular functions, and cellular components of core targets. (F) KEGG enrichment analysis of effect targets of pathways modulated by DSY compounds.
Abbreviations: CC: Cellular component; DS: *Salvia miltiorrhiza Bge.*; DSY: Dan-Shen-Yin; GO: Gene Ontology; IL2: Interleukin 2; IL6: Interleukin 6; JAK: Janus kinase; KEGG: Kyoto Encyclopedia of Genes and Genomes; MAPK: Mitogen-activated protein kinase; MF: Molecular function; NF-κB: Nuclear factor kappa B; PPI: Protein–protein interaction; STAT3: Signal transducer and activator of transcription 3; SR: *Amomum villosum Lour.*; TNF: Tumor necrosis factor; TP53: Tumor protein p53; TX: *Santalum album L.*

Table 5. Degree, betweenness, and closeness values of potential bioactive compounds in DSY targeting gastritis

Serial number	Compound name	Degree	Betweenness	Closeness	Sources
LCDSY-3	Citric acid	92	33661.1680	0.1223	DSY, DS
LCDSY-31	Rosmarinic acid	28	7463.3510	0.1155	DSY, DS
LCDSY-45	Tanshinone IIA	25	6402.2240	0.1144	DSY, DS
LCDSY-14	Caffeic acid	24	6760.6210	0.1158	DSY, DS
LCDSY-11	Epicatechin	24	5167.0913	0.1149	DSY, SR
LCDSY-46	Cryptotanshinone	16	2765.5713	0.1143	DSY, DS
LCDSY-29	Salvianolic acid B	16	5837.8240	0.1124	DSY, DS
LCDSY-6	Danshensu	13	2847.7444	0.1134	DSY, DS
LCDSY-15	Catechin	12	1437.6676	0.1137	DSY, SR
LCDSY-43	Isocryptotanshinone	11	1593.7957	0.1137	DSY, DS
LCDSY-42	Neocryptotanshinone	10	803.9311	0.1137	DSY, DS
LCDSY-9	Protocatechuic acid	9	1740.7864	0.1136	DSY, DS, SR
LCDSY-7	Vanillin	8	1034.0078	0.1136	DSY, TX
LCDSY-20	Salvianolic acid A	7	509.3273	0.1121	DSY, DS
LCDSY-10	3,4-Dihydroxyhydrocinnamic acid	7	717.6403	0.1128	DSY, DS
LCDSY-8	Vanillic acid	7	737.9602	0.1135	DSY, SR
LCDSY-12	Protocatechualdehyde	6	1142.4958	0.1123	DSY, DS, SR
GCDSY-8	Isovanillin	5	471.3908	0.1132	DSY, DS
GCDSY-7	Bornyl acetate	4	600.2523	0.1105	DSY, SR, TX
GCDSY-15	Diepicedrene-1-oxide	3	515.2957	0.1034	DSY, TX
GCDSY-3	Benzeneacetaldehyde	3	461.9877	0.1066	DSY, SR, DS
GCDSY-13	Cryptomeridiol	2	15.5880	0.1101	DSY, DS

Notes: Degree refers to the number of connections to other nodes in the network. Betweenness refers to the frequency of a node appearing on shortest paths between nodes. Closeness refers to the average shortest path from the node to all other nodes.
Abbreviations: DS: *Salvia miltiorrhiza Bge.*; DSY: Dan-Shen-Yin; SR: *Amomum villosum Lour.*; TX: *Santalum album L.*

binding transcription factor binding, cytokine activity, and protein kinase activity were enriched.

As shown in Figure 8F, the KEGG enrichment analysis indicated that 10 out of the top 20 pathways (total = 170 pathways) were associated with inflammation. These include lipid and atherosclerosis, fluid shear stress and atherosclerosis, MAPK signaling pathway, JAK-STAT signaling pathway, inflammatory bowel disease, nuclear factor-kappa B (NF-κB) signaling pathway, p53 signaling pathway, rheumatoid arthritis, leukocyte transendothelial migration, and cell cycle. A disease-core target-compound-pathway network constructed using Cytoscape 3.9.1 exhibited 134 nodes and 346 edges (Figure 8F). This network illustrates that one compound can act on multiple targets while multiple compounds act on a common target, and the targets are involved in different signaling pathways.

In summary, this study employed network pharmacology analysis based on the comprehensive characterization of DSY decoction, thereby elucidating its active compounds, core targets, and associated pathways involved in the treatment of gastritis. The analysis identified 22 bioactive compounds, potentially representing the key material basis by which DSY exerts its therapeutic effects. At present, most of these compounds have been previously reported in pharmacological studies to exhibit a range of activities relevant to the treatment of gastritis. For instance, rosmarinic acid has a significant gastric protective effect as it increases antioxidant defense and PGE_2 secretion.[31] Hiruma Lima *et al.*[32] found that Epi present in *Virola surinamensis* resin exhibits anti-ulcer activity. Catechin and isocryptotanshinone have the potential preventive effects against gastric carcinogenesis.[33,34] Cheng *et al.*[35] proposed that protocatechuic acid can treat oxidative stress-associated gastrointestinal ulcer diseases by inducing Parkinson disease protein 7 (DJ-1) expression. The results of Murakami *et al.*[36] indicated that salvianolic acid A shows antisecretory and anti-ulcer activity by inhibiting the gastric H^+, K^+-ATPase. Ren *et al.*,[37] using a rat model of chronic atrophic gastritis (CAG), demonstrated that tanshinone IIA may alleviate inflammation and cellular apoptosis by inhibiting the activation of the JAK2/

STAT3 signaling pathway and the nuclear translocation of NF-κB, thereby mitigating structural and functional damage to the gastric mucosa. Yang *et al.*[38] demonstrated that caffeic acid attenuates hydrochloric acid/ethanol-induced gastric inflammatory responses by inhibiting the JNK, IRAK1, and IRAK4 signaling pathways in a murine model. In addition, numerous studies have shown that Cry, salvianolic acid B, danshensu, neocryptotanshinone, vanillin, vanillic acid, and bornyl acetate have significant anti-inflammatory activities.[39-46] These findings suggest that DSY has a substantial material basis for the prevention and treatment of gastritis and its progression to gastric cancer. Moreover, the constructed disease-core target-compound-pathway interaction network suggests that DSY exerts its therapeutic effects through multiple targets and signaling pathways, which may underlie its notable clinical efficacy. Half of the top 20 pathways analyzed by KEGG enrichment were associated with inflammation. Among them, MAPK signaling pathway, NF-κB signaling pathway, p53 signaling pathway, and JAK-STAT signaling pathway are common signaling pathways targeted in CAG treatment.[47,48] In addition, previous studies have shown that pathways associated with inflammatory bowel disease, rheumatoid arthritis, leukocyte transendothelial migration, and cell cycle are strongly associated with gastritis caused by *H. pylori*.[49-52] These findings further demonstrate that DSY can effectively alleviate and protect against inflammatory injury of the gastric mucosa, thereby preventing or treating gastritis.

4. Conclusion

Clinical studies have shown that DSY demonstrates notable efficacy in the treatment of gastritis. As a multi-component compound preparation, DSY contains diverse chemical constituents, and reliance on a single detection method is insufficient to comprehensively elucidate its material basis. Therefore, this study characterized the nonvolatile compounds, volatile compounds, and polysaccharides in DSY decoction using UHPLC-Orbitrap Exploris MS, HS-GC-MS, and HPLC. Fifteen volatile and fifty-two nonvolatile compounds were identified in the DSY decoction, primarily originating from TX and DS. In addition, polysaccharides in the DSY decoction, primarily derived from SR and DS, consisted mainly of galactose, glucose, and galacturonic acid. Finally, based on a comprehensive characterization of DSY decoction, network pharmacology analysis identified 22 active compounds interacting with 55 core targets and modulating 10 inflammation-related signaling pathways, thereby elucidating the potential mechanisms underlying the therapeutic effects of DSY in treating gastritis. However, this study lacks a systematic quality assessment of DSY and does not include an analysis of its blood-absorbed (bioavailable) compounds. Quantifying the therapeutic efficacy by using selected active compounds as quality control markers can substantially improve the accuracy and reliability of DSY's quality evaluation. This study provides references and a basis for the development of such evaluation methods for DSY in the future. In addition, as a multi-component compound preparation, the mechanisms through which DSY treats gastritis and prevents its progression to gastric cancer warrant further investigation.

Acknowledgments

None.

Funding

This study was supported by the Science and Technology Program of Tianjin, China (Grant numbers: 24ZYJDSS00310 and 24ZYJDSS00300).

Conflict of interest

Miaomiao Jiang is an Editorial Board Member of this journal, but was not in any way involved in the editorial and peer-review process conducted for this paper, directly or indirectly. Separately, other authors declared that they have no known competing financial interests or personal relationships that could have influenced the work reported in this paper.

Author contributions

Conceptualization: Miaomiao Jiang
Formal analysis: Miaomiao Jiang, Jianbing Dong, Zhirong Zhou
Investigation: Jianbing Dong, Zhirong Zhou
Methodology: Jianbing Dong, Zhirong Zhou, Peng Lei
Writing–original draft: Jianbing Dong, Zhirong Zhou, Yi Chen
Writing–review & editing: Jianbing Dong, Zhirong Zhou, Yi Chen, Qingrui Zhang

Ethics approval and consent to participate

Not applicable.

Consent for publication

Not applicable.

Availability of data

Data is available from the corresponding author upon reasonable request.

References

1. Wafaey AA, El-Hawary SS, Abdelhameed MF, *et al.* Green synthesis of zinc oxide nanoparticles using ethanolic extract of *Gliricidia sepium* (Jacq.) kunth. Ex. Walp.,

stem: Characterizations and their gastroprotective effect on ethanol-induced gastritis in rats. *Bioorg Chem*. 2024;145:107225.

doi: 10.1016/j.bioorg.2024.107225

2. Gao X, Yin P, Ren Y, *et al*. Predicting personalized diets based on microbial characteristics between patients with superficial gastritis and atrophic gastritis. *Nutrients*. 2023;15(22):4738.

doi: 10.3390/nu15224738

3. López MJ, Carbajal J, Alfaro AL, *et al*. Characteristics of gastric cancer around the world. *Crit Rev Oncol Hematol*. 2023;181:103841.

doi: 10.1016/j.critrevonc.2022.103841

4. Li JX, Chen J, Lu B, Wang YG. Consensus on diagnosis and treatment of chronic atrophic gastritis with integrated traditional Chinese and western medicine (2017). *Chin J Integr Tradit West Med Dig*. 2018;26(2):121-131.

doi: 10.3969/j.issn.1671-038X.2018.02.03

5. Du LJ, Chen BR, Kim JJ, Kim S, Shen JH, Dai N. Helicobacter pylori eradication therapy for functional dyspepsia: Systematic review and meta-analysis. *World J Gastroenterol*. 2016;22(12):3486-3495.

doi: 10.3748/wjg.v22.i12.3486

6. Li Z, Wu C, Li L, *et al*. Effect of long-term proton pump inhibitor administration on gastric mucosal atrophy: A meta-analysis. *Saudi J Gastroenterol*. 2017;23(4):222-228.

doi: 10.4103/sjg.SJG-573-16

7. Liu M, Li Z, Yue O, *et al*. Material basis and integrative pharmacology of danshen decoction in the treatment of cardiovascular diseases. *Phytomedicine*. 2023;108:154503.

doi: 10.1016/j.phymed.2022.154503

8. Yu ZH. Observation on the therapeutic effect of modified danshen yin on chronic gastritis. *Chin J Clin Ration Drug Use*. 2012;5(4):86-87.

doi: 10.15887/j.cnki.13-1389/r.2012.04.017

9. Sun XN, Su YQ, Xu XQ, Zhao CP, Ji JL, Sun B. Treating gastric collaterals obstructed type of chronic gastritis with the danshen decoction by professor sun bin. *Clin J Chin Med*. 2021;13(14):69-72.

doi: 10.3969/j.issn.1674-7860.2021.14.020

10. Wang Df, Zhao M, Dong XY, Li XY. Clinical effect and mechanism of modified danshenyin against chronic atrophic gastritis with syndrome of stasis in stomach collateral: Based on theory of collateral diseases. *Chin J Exp Tradit Med Form*. 2022;28(23):122-127.

doi: 10.13422/j.cnki.syfjx.20221623

11. Li J, Chai JB. Experimental study on the mechanism of danshen yin in preventing pyloric ligation induced gastric ulcer in rats. *Chin Arch Tradit Chin Med*. 2006;(4):588-589.

doi: 10.3969/j.issn.1673-7717.2006.04.003

12. Zhang HQ, Liu L. Effects and mechanisms of danshenyin on accelerate gastric ulcer healing. *Chin J Clin Pharmacol Ther*. 2005;(7):812-818.

doi: 10.3969/j.issn.1009-2501.2005.07.022

13. Liu MN, Yuan G, Luo G, *et al*. Network pharmacology analysis and experimental verification strategies reveal the action mechanism of danshen decoction in treating ischemic cardiomyopathy. *Evid Based Complement Alternat Med*. 2022;2022:7578055.

doi: 10.1155/2022/7578055

14. Jing YS, Ma YF, Wang FF, Zhang YW, Wu LF, Zhang DS. Research progress on content determination, structural characterization and pharmacological activity of *Salvia miltiorrhiza* polysaccharides. *China Pharm*. 2020;31(16):2037-2042.

doi: 10.6039/j.issn.1001-0408.2020.16.22

15. Shan XX, Hong BZ, Liu J, *et al*. Review of chemical composition, pharmacological effects, and clinical review of chemical composition, pharmacological effects, and clinical. *China J Chin Mater Med*. 2021;46(21):5496-5511.

doi: 10.19540/j.cnki.cjcmm.20210630.203

16. Yang DS, Zhang Y, Shu Y, Cao H. Research progress on chemical constituents and pharmacological effects of *Amomum villosum*. *Guangdong Chem Ind*. 2022;49(8):111-114.

doi: 10.3969/j.issn.1007-1865.2022.08.035

17. Zhang W, Liu YY, Zou YC, Yu M, Zhan ZL, Xin GS. Advances on the investigation of phytochemistry and pharmacological activities of heartwood of *Santalum album* L. *World Sci Technol Modernization Tradit Chin Med*. 2020;22(12):4300-4307.

doi: 10.11842/wst.20200407016

18. Navarini L, Gilli R, Gombac V, Abatangelo A, Bosco M, Toffanin R. Polysaccharides from hot water extracts of roasted *Coffea arabica* beans: Isolation and characterization. *Carbohydr Polym*. 1999;40(1):71-81.

doi: 10.1016/S0144-8617(99)00032-6

19. Dubois M, Gilles KA, Hamilton JK, Rebers PA, Smith F. Colorimetric method for determination of sugars and related substances. *Anal Chem*. 1956;28(3):350-356.

doi: 10.1021/ac60111a017

20. Blumenkrantz N, Asboe-Hansen G. New method for quantitative determination of uronic acids. *Anal Biochem*. 1973;54(2):484-489.

doi: 10.1016/0003-2697(73)90377-1

21. Lowry OH, Rosebrough NJ, Farr AL, Randall RJ. Protein

measurement with the folin phenol reagent. *J Biol Chem*. 1951;193(1):265-275.

doi: 10.1016/S0021-9258(19)52451-6

22. Sun X, Wang H, Han X, Chen S, Zhu S, Dai J. Fingerprint analysis of polysaccharides from different *Ganoderma* by HPLC combined with chemometrics methods. *Carbohydr Polym*. 2014;114:432-439.

doi: 10.1016/j.carbpol.2014.08.048

23. Guo JS, Liu HY, Huang XJ, Zhang M, Chen J, Nie ZW. Effect of the different extracts of santali albi lignum on isolated the small intestine movement function and gastric emptying of mice. *Chin J Exp Tradit Med Form*. 2012;18(2):139-143.

doi: 10.3495/R.2011116.1422.001

24. Zhang HF, Xue YW. Empirical study in the relation of gastric mucosal lesion with gastric emptying and gastric acid secretion. *Zhonghua Wei Chang Wai Ke Za Zhi*. 2008;11(5):472-476.

25. Li J, Ren XJ, Lou Y. Research progress on the pathogenesis of gastric cancer induced by bile acids and the potential effects of *Salvia miltiorrhiza* extract. *J Chin Foreign Med Pharm Res*. 2024;3(8):156-158.

doi: 10.3969/j.issn.2096-6229.2024.08.052

26. Miao HX, Zhang HW, Wang J. Research progress on pharmacological mechanism of *Salvia miltiorrhiza* and its extracts in the treatment of oral malignant tumors. *Glob Tradit Chin Med*. 2023;16(3):565-570.

doi: 10.3969/j.issn.1674-1749.2023.03.038

27. Yu YY, Zhu YY, Zhang SC, *et al*. Research progress of plant polysaccharides in treatment of gastrointestinal diseases. *Chin Arch Tradit Chin Med*. 2024;42(4):194-199.

doi: 10.13193/j.issn.1673-7717.2024.04.038

28. Li L, Lan X, Peng X, *et al*. Polysaccharide from *Salviae miltiorrhizae* radix et rhizoma attenuates the progress of obesity-induced non-alcoholic fatty liver disease through modulating intestinal microbiota-related gut-liver axis. *Int J Mol Sci*. 2022;23(18):10620.

doi: 10.3390/ijms231810620

29. Gao BQ, Liu Y, Chen YH, Yang DC, Liu GP. Characteristics of gut microbiota in patients with chronic atrophic gastritis. *Chin J Microecol*. 2024;36(3):282-291.

doi: 10.3389/fcimb.2019.00369

30. Liu H, Zhuang S, Liang C, *et al*. Effects of a polysaccharide extract from *Amomum villosum* lour. on gastric mucosal injury and its potential underlying mechanism. *Carbohydr Polym*. 2022;294:119822.

doi: 10.1016/j.carbpol.2022.119822

31. Heidari F, Komeili-Movahhed T, Hamidizad Z, Moslehi A. The protective effects of rosmarinic acid on ethanol-induced gastritis in male rats: Antioxidant defense enhancement. *Res Pharm Sci*. 2021;16(3):305-314.

doi: 10.4103/1735-5362.314829

32. Hiruma-Lima CA, Batista LM, Almeida AB, *et al*. Antiulcerogenic action of ethanolic extract of the resin from *Virola surinamensis* warb. (*Myristicaceae*). *J Ethnopharmacol*. 2009;122(2):406-409.

doi: 10.1016/j.jep.2008.12.023

33. Chen ZM, Huang L, Li MM, Meng L, Ying SC, Xu AM. Inhibitory effects of isocryptotanshinone on gastric cancer. *Sci Rep*. 2018;8(1):9307.

doi: 10.1038/s41598-018-27638-0

34. Ohno T, Ohtani M, Suto H, *et al*. Effect of green tea catechins on gastric mucosal dysplasia in insulin-gastrin mice. *Oncol Rep*. 2016;35(6):3241-3247.

doi: 10.3892/or.2016.4717

35. Cheng YT, Lin JA, Jhang JJ, Yen GC. Protocatechuic acid-mediated DJ-1/PARK7 activation followed by PI3K/mTOR signaling pathway activation as a novel mechanism for protection against ketoprofen-induced oxidative damage in the gastrointestinal mucosa. *Free Radic Biol Med*. 2019;130:35-47.

doi: 10.1016/j.freeradbiomed.2018.10.415

36. Murakami S, Kijima H, Isobe Y, *et al*. Effect of salvianolic acid a, a depside from roots of *Salvia miltiorrhiza*, on gastric H+,K(+)-ATPase. *Planta Med*. 1990;56(4):360-363.

doi: 10.1055/s-2006-960982

37. Ren L, Wang LM, Zhang M. Study on the mechanism of tanshinone IIA alleviates gastric mucosal injury in rats with chronic atrophic gastritis by inhibiting JAK2/STAT3 pathway. *Tianjin J Tradit Chin Med*. 2024;41(7):914-921.

doi: 10.11656/j.issn.1672-1519.2024.07.19

38. Yang WS, Jeong S, Yi YS, *et al*. IRAK1/4-targeted anti-inflammatory action of caffeic acid. *Mediators Inflamm*. 2013;2013:518183.

doi: 10.1155/2013/518183

39. Ciciliato MP, Souza MCD, Tarran CM, Castilho ALTD, Vieira AJ, Rozza AL. Anti-inflammatory effect of vanillin protects the stomach against ulcer formation. *Pharmaceutics*. 2022;14(4):755.

doi: 10.3390/pharmaceutics14040755

40. Guo R, Li L, Su J, *et al*. Pharmacological activity and mechanism of tanshinone IIA in related diseases. *Drug Des Devel Ther*. 2020;14:4735-4748.

doi: 10.2147/dddt.s266911

41. Li J, Chen YH, Li LZ, *et al*. Omics and transgenic analyses reveal that salvianolic acid b exhibits its anti-inflammatory effects through inhibiting the mincle-syk-related pathway in

macrophages. *J Proteome Res*. 2021;20(7):3734-3748.

doi: 10.1021/acs.jproteome.1c00325

42. Wu C, Zhao W, Zhang X, Chen X. Neocryptotanshinone inhibits lipopolysaccharide-induced inflammation in RAW264.7 macrophages by suppression of NF-κB and iNOS signaling pathways. *Acta Pharm Sin B*. 2015;5(4):323-329.

doi: 10.1016/j.apsb.2015.01.010

43. Wu YH, Wu YR, Li B, Yan ZY. Cryptotanshinone: A review of its pharmacology activities and molecular mechanisms. *Fitoterapia*. 2020;145:104633.

doi: 10.1016/j.fitote.2020.104633

44. Yoo SR, Jeong SJ, Lee NR, Shin HK, Seo CS. Simultaneous determination and anti-inflammatory effects of four phenolic compounds in dendrobii herba. *Nat Prod Res*. 2017;31(24):2923-2926.

doi: 10.1080/14786419.2017.1300798

45. Zhang J, Zhang Q, Liu G, Zhang N. Therapeutic potentials and mechanisms of the Chinese traditional medicine danshensu. *Eur J Pharmacol*. 2019;864:172710.

doi: 10.1016/j.ejphar.2019.172710

46. Zhang T, Lu SH, Bi Q, *et al*. Volatile oil from amomi fructus attenuates 5-fluorouracil-induced intestinal mucositis. *Front Pharmacol*. 2017;8:786.

doi: 10.3389/fphar.2017.00786

47. Jia JH, Zhao H, Li F, *et al*. Research on drug treatment and the novel signaling pathway of chronic atrophic gastritis. *Biomed Pharmacother*. 2024;176:116912.

doi: 10.1016/j.biopha.2024.116912

48. Liu X, Wang S, Li J, Zhang J, Liu D. Regulatory effect of traditional Chinese medicines on signaling pathways of process from chronic atrophic gastritis to gastric cancer. *Chin Herb Med*. 2022;14(1):5-19.

doi: 10.1016/j.chmed.2021.10.008

49. Nagura H, Ohtani H, Sasano H, Matsumoto T. The immuno-inflammatory mechanism for tissue injury in inflammatory bowel disease and helicobacter pylori-infected chronic active gastritis. Roles of the mucosal immune system. *Digestion*. 2001;63 Suppl 1:12-21.

doi: 10.1159/000051905

50. Nakamura H, Mukai E, Hirano D, Matsuhisa T, Yamada N, Yoshino S. Gastrointestinal disorder and helicobacter pylori infection in patients with rheumatoid arthritis. *Mod Rheumatol*. 2001;11(1):23-27.

doi: 10.3109/s101650170039

51. Polat A, Cinel L, Dusmez D, Aydin O, Egilmez R. Expression of cell-cycle related proteins in helicobacter pylori gastritis and association with gastric carcinoma. *Neoplasma*. 2002;49(2):95-100.

doi: 10.1038/sj.neo.7900211

52. Suzuki T, Ina K, Nishiwaki T, *et al*. Differential roles of interleukin-1beta and interleukin-8 in neutrophil transendothelial migration in patients with helicobacter pylori infection. *Scand J Gastroenterol*. 2004;39(4):313-321.

doi: 10.1080/00365520310008610